Milli-sized calcium alginate sorbent supporting the dye waste – calcium fluoride hybrid for adsorption of organic contaminants†

Dan-Hua Zhao,[a] Yu-Lin Shen,[a] Ya-Lei Zhang,*[b] De-Quan Wei,[a] Nai-Yun Gao[a] and Hong-Wen Gao*[a]

Received 6th November 2009, Accepted 20th January 2010
First published as an Advance Article on the web 26th February 2010
DOI: 10.1039/b923340g

A new kind of milli-sized sorbent—calcium alginate supporting a weak acidic pink red B (APRB)–calcium fluoride nano-sized hybrid—was prepared. The micro-structure of the hybrid and adsorbent were characterized, and its adsorption capacity for organic contaminants, *e.g.* dyes, PCBs and microcystin (MC)-LR, was investigated. Cationic dyes were adsorbed selectively *via* charge attraction, with a saturation capacity of 188 mg of cationic red 3R per gram of the milli-sized adsorbent. However, the adsorptions of PCBs and MC-LR corresponded to the octanol–water partition law, and their partition coefficients were calculated to be 7788.6 mg kg^{-1} for PCB029, 13325 mg kg^{-1} for PCB101, 434.6 mg kg^{-1} for PCB180, and 369.2 mg kg^{-1} for MC-LR. When the milli-sized adsorbent was used in the treatment of two concentrated dye wastewaters and two polluted ground waters, the removal of the colored substances, chemical oxygen demand (COD), and concentration of PCBs and MC-LR were satisfactory. In the synthesis of the materials, all of the reactants are easily available and harmless to the environment, and APRB may be obtained from concentrated APRB-containing wastewater instead. The development of the milli-sized hybrid adsorbent provided liquid–solid separation, for favorable use in engineering. It will play an important role in the treatment of concentrated wastewater and the remediation of ground water contamination.

Introduction

A worldwide thriving and prosperous economy has simultaneously resulted in severe environmental pollution.[1] Plenty of domestic sewage and industrial wastewater is discharged into various surface water bodies *e.g.* lakes, rivers and seas, especially in developing countries.[2] The organic contamination and eutrophication are rather serious in some natural water bodies, such that the water quality/function gets worse and worse.[3] For example, there were various toxic pollutants, *e.g.* pharmaceuticals and personal care products (PPCPs), persistent organic pollutants (POPs),[4] endocrine disrupting chemicals (EDCs), and algae toxins[5], discovered in the aquatic bodies around the Yangtze River Delta region, which is the most developed area of China. As a well-known case, the blue-green algae outbreak in Taihu Lake caused a drinking water crisis for cities in the Delta in 2006.[6] The primary measure is to strengthen pollution source control, implement wastewater treatment, and reduce the emissions of pollutants, so as to solve the problem of water body pollution. The conventional treatment techniques, such as flocculation, adsorption, ion exchange, membrane filtration, oxidation, electrolysis, and so on, have been applied extensively to the treatment of wastewater.[7] However, some of these techniques often have serious limitations.[8] The joint use of a variety of techniques is essential to achieve the discharge requirements for organic wastewater, greatly increasing the process cost, and secondary pollution may appear. As an environmentally friendly approach to treating wastewater, "using waste to treat waste" is what people have aspired to, with waste reuse being an optimal selection.[9] On the other hand, the *in situ* remediation of polluted water bodies can be performed to restore water body function. In most cases, the water remediation is carried out by biological or ecological technology, such as wetland construction, microorganisms, super-rich aquatic plants, control of water soil loss, *etc.*[10]

Various synthesis techniques developed in the last few years gave access to hybrid materials.[11] By means of inorganic/organic hybrid methods, our group has synthesized some new adsorbents with dye waste, which were applied to the treatment of concentrated organic wastewaters.[12] Although they have high adsorption capacity, solid–liquid separation is difficult in use. In order to solve the problem for engineering applications, the immobilization of the hybrid material on an easily separated carrier was studied. As a natural polysaccharide extracted from brown seaweeds, alginate is a common and well-known support material.[13] In the present work, a new type of nano-sized hybrid material was synthesized by hybridizing weak acid pink red B (APRB) from dye wastewater into calcium fluoride (Fig. 1 A–B), which was then immobilized in the milli-sized calcium alginate globes (Fig. 1 C). The adsorption of ionic dyes, POPs and algae toxins onto the milli-sized adsorbent was investigated. The globes may be made into drift blankets spread on to the water surface (Fig. 1 D-1) or fixed on to the bottom of ships (Fig. 1 D-2) for the *in situ* cleaning of organic pollutants.

[a]*State Key Laboratory of Pollution Control and Resource Reuse, College of Environmental Science and Engineering, Tongji University, Shanghai - 200092, China. E-mail: hwgao@tongji.edu.cn; Fax: (+) 86-21-65988598*
[b]*Institute of Modern Agricultural Science and Engineering, Tongji University, Shanghai - 200092, China. E-mail: zhangyl@tongji.edu.cn*
† Electronic supplementary information (ESI) available: Fig. S1–S18 and Table S1. See DOI: 10.1039/b923340g

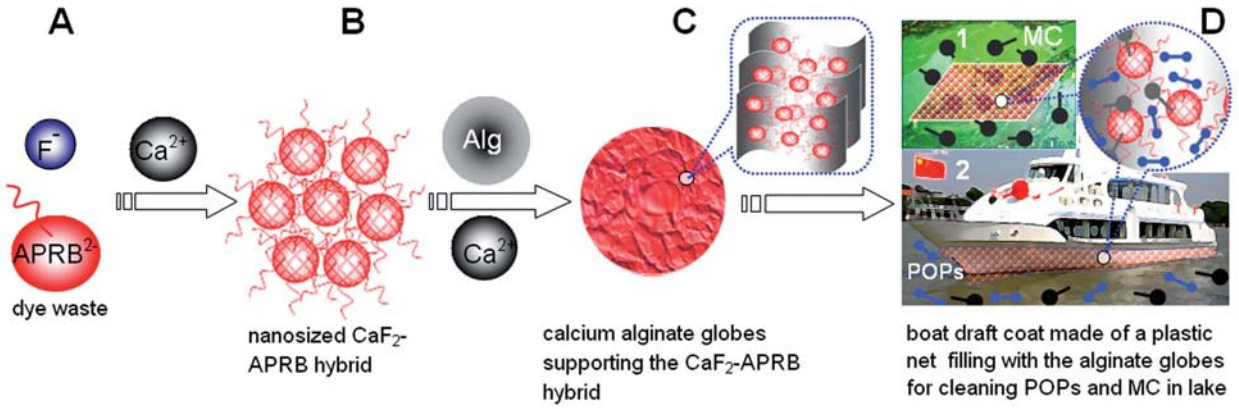

Fig. 1 Cartoon illustration of the formed particle structure, and simultaneous capture of POPs mixture and MC-LR.

Experimental

Apparatus and materials

A photodiode array spectrometer (Model S4100, Scinco, Korea) with the Labpro plus software (Firmware Version 060105) was used to determine the concentration of colored compounds. A model analyst 400 atomic absorption spectrophotometer (Perkin-Elmer Instruments, USA) was used to determine the calcium content in the hybrid material. An electrochemical work station (Model LK2006, Lanlike chemical electronic high technology Co., Ltd., Tianjin, China) was used to determine flouride in the CaF_2–APRB hybrid material (CFA). Infrared (IR) spectra of the hybrid powder were measured by an infrared spectrometer system (Model Equinoxss/hyperion 2000, Bruker Co., Germany). A vacuum freeze dryer (Model LGJ, Ningbo scientz Co. Ltd., China) was used to remove water from the calcium alginate-only (CA) and calcium alginate supporting CaF_2–APRB hybrid (CASCA) wet beads. Scanning electronic microscopy (SEM) (Model Quanta 200 FEG, FEI Co., USA) was used to measure the size and shape of the materials. Element analysis and microstructure of the materials were conducted with a high resolution transmission electronic microscope (HRTEM) (Model Tecnai G^2 F20 S-Twin, FEI Co., USA) (120 kV, 2.4 Å resolution) equipped with an energy dispersive spectroscopy X-ray (EDX). The thermal gravimetric analysis (TGA) of the powder material was carried out with a thermogravimetry (Model TAQ 600, USA). The surface area, pore size, and pore volume of CFA, CASCA and CA were determined by N_2 adsorption/desorption isotherms obtained at −195.7 °C on a Micrometric ASAP 2020 analyzer (American), and pore size distributions were calculated using the Barret–Joyner–Halenda (BJH) model on the desorption branch. High performance liquid chromatography (HPLC) (Model L-2000, Hitachi, Japan) was used to determine PCBs and MC-LR with a diode array detector (DAD) (Model L-2455) and an inverse-phase column (C18, Model Allsphere ODS-2 5μ, 250 mm × 4.6 mm, Alltech Associates, Inc., USA). A programmable digestion system (Model 5B-1, Lanzhou, China) and a portable chemical oxygen demand (COD) analyzer (Model PORS-15V, Pgeneral Co., China) were coupled for determination of COD in wastewater.

The APRB reagent (content >98%, C.I. 18073) was purchased from Sigma and an APRB-containing wastewater (pH 8.6), containing 0.074% APRB, was provided by Jinhua Shuanghong Chemical Plant (Zhejiang, China), which were used to prepare the hybrid material. Cationic dyes: ethyl violet (EV, C.I. 42600), methylene blue (MB, C.I. 52015), cationic red 3R (CR3R, C.I. 48013), basic brilliant blue BO (BBBO, C.I. 42595) and victoria blue B (VBB, C.I. 44045), and anionic dyes: reactive brilliant red K-2BP (RBRK-2BP, C.I. 18208), weak acid green GS (WAGGS, C.I. 61580), reactive brilliant red X-3B (RBRX-3B, C.I. 18200), acid brilliant blue 6B (ABB6B, C.I. 42660) and mordant blue 9 (MB-9, C.I. 14855) (all content >95%) were purchased from Sigma. PCBs: 2,4,5-trichlorobipehenyl (PCB029) and 2,2′,4,5,5′-pentachlorobiphenyl (PCB101) and 2,2′,3,4,4′,5,5′-heptachlorobiphenyl (PCB180) were purchased from J&K Chemicals (>95%). Microsystin-LR (MC-LR, 995.2 Da) was purchased from Zen-U Biotechnology Co (Taiwan, 95–99%). Sodium alginate powder and calcium chloride were purchased from Sinopharm Chemical Reagents (Shanghai, China). NaF was purchased from Shanghai Medical Group. Two dye wastewaters (1# and 2#, unknown dye names) were sampled from Jinjiang Chemical (Hangzhou, China) and Xingwu Dye Plant (Nantong, China). Their color strengths were determined to be 137620 (#1 - red) and 46400 (#2 - blue) by spectrophotometry and their CODs to be 3320 (#1) and 1156 mg L^{-1} (#2) by COD analyzer. A PCB-polluted water sample (#3) containing PCB029, PCB101 and PCB180, and an MC-LR polluted water sample (#4) mixed with PCB101 were prepared with the Taihu Lake water.

Preparation and measurement of the materials

Into an APRB solution (1.2 mmol L^{-1}), prepared with the APRB reagent or the APRB-containing wastewater mixed with 0.040 mol L^{-1} NaF, 200 mL of 0.016 mol L^{-1} $CaCl_2$ was added slowly under stirring. The reaction liquid was stewed for precipitating the suspending substances, and then the precipitate was washed three times with 2000 mL of deionized water. The final suspending substance liquid with the CaF_2–APRB hybrid (CFA) material was formed. The CFA material was dissolved into 0.1 mol L^{-1} EDTA, and the APRB, Ca and F concentrations were determined by spectrophotometry, AAS and ion selective electrode methods. Thus, the composition ratio of the hybrid material was calculated. The microstructure of the material was measured by TGA, XRD, IR, SEM and TEM-EDX.

400 mL of a precursor liquid was prepared by mixing 0.1 mol L^{-1} sodium alginate with 70 mL of the above CFA-suspending substance liquid (6.0%, w/v solution). The mixture was stirred strongly for 1 h, and then it was dripped into 0.18 mol L^{-1} $CaCl_2$ 400 mL solution with an injection column at a constant speed of approximately 4.5 mL min^{-1}. The spherical CASCA adsorbent was formed. Finally, the globes were kept in the same calcium solution for 1 h so that the gelation reaction had enough time to complete. After the curing period, the beads were washed with distilled water and stored in distilled water to remove the unreacted calcium from the beads' surface. Excess water on the surface of the beads was removed by filter paper immediately before use for the experiments. The CA beads were prepared according to the above same method. The extent of drying of CA and CASCA were determined by measuring the weight loss after they were dried in an oven at 110 °C for 6 h. The extent of drying was (1.21 ± 0.04)% for CA and (2.87 ± 0.06)% for CASCA. The surface and internal structure of wet CA and CASCA adsorbents after freeze-drying for 24 h were determined using a scanning electron microscope. Micro-particle size and size distribution were measured by analyzing the SEM photomicrographs.

Adsorption of organic compounds

Ten dye solutions were prepared which were five anionic dyes (all 100 μmol L^{-1}): WAGGS, ABB6B, MB-9, RBRX-3B and RBRK-2BP, and five cationic dyes (all 100 μmol L^{-1}): EV, MB, CR3R, BBBO and VBB. All of them were treated with 0.4% of CFA. The color change of the supernatants was compared with that of the corresponding dye solution for the adsorption selectivity. Four cationic dyes: BBBO, CR3R, EV and MB were selected as the adsorbates for investigating the adsorption mechanism of the materials. Into a series of 10 mL dye solutions from 25.0 to 300.0 μmol L^{-1}, 4.0 mg of CFA was added. After mixing for 15 min, the liquids were centrifuged at 11000 rpm for 10 min and the dye concentration in the supernatants was determined by spectrophotometry. Thus, the molar ratio, γ, of dye binding to the material was calculated. According to the same method, the CA or CASCA was added to the CR3R solutions as a representative of the cationic dyes. Then, the mixing bottle was oscillated for 3 h in a mechanical shaker. The adsorptions of the cationic dyes used were carried out with CA and CASCA.

In order to clarify the adsorption of hydrophobic organic contaminants on to the milli-sized sorbent, PCB029, PCB101, PCB180 and MC-LR were selected. A known weight of CFA was added to 10 mL of each PCB and MC-LR solutions in various concentrations, and each liquid was mixed for 15 min. According the same method, the CA or CASCA was added in the PCB and MC-LR solutions, but the mixing bottle was oscillated for 3 h in a mechanical shaker. Then, the concentrations of PCBs and MC-LR in the supernatants were determined by HPLC coupled with a DAD at 210 nm for PCBs, and 238 nm for MC-LR. The optimized mobile phases were methanol–phosphate buffer (pH 7.0) (v/v: 95 : 5) with the flow rate at 1.0 mL min^{-1} (isocratic mode) for PCBs, and methanol–water (v/v: 80 : 20) with the flow rate at 0.6 mL min^{-1} for MC-LR. The retention time is 3.75 min for PCB029, 4.21 min for PCB101, 7.10 min for PCB180 and 5.08 min for MC-LR. All injections (20.0 μL) were performed manually. Their partition coefficients (K_{pw}) on the sorbent particles were calculated, and the relationship between the octanol/water partition coefficient (K_{ow}) and K_{pw} of the contaminants was established.

Treatment and restoration of polluted waters

The treatment of two cationic dye wastewaters (#1 and #2, unknown dye names) was carried out by adding the adsorbents (0.35, 0.70, 1.05, 1.40 and 1.75 mL of 6% CFA liquid, 1.0, 3.0, 5.0, 8.0 and 10.0 g of wet CA and CASCA in 20 mL of each solution). The bottles were placed in a mechanical shaker and oscillated for 3 h. The color strength of the supernatants was measured by spectrophotometry at 535 nm for sample #1 and 651 nm for sample #2, and the COD determined with a rapid COD analyzer. By the same method, two polluted waters, sample #3 containing PCB029, PCB101 and PCB180, and the other sample (#4) containing PCB101 and MC-LR were treated with the milli-sized sorbent. The concentrations of PCBs and MC-LR in the supernatants were determined by HPLC.

Results and discussion

Formation and characterization of the CaF_2–APRB hybrid material

The hybridization of APRB into CaF_2 particles remained maximal when the molar ratio of Ca^{2+} to F^- was approximately 0.4 (refer to the ESI,† Fig. S1). From the effect of pH on the hybridization of APRB (refer to the ESI,† Fig. S2), the CaF_2 dissolved when the pH was less than 2. Thus, the preparation of the hybrid material was carried out in neutral media. According to the optimal conditions, a suspending solid (SS) liquid containing CFA was synthesized. After the SS liquid was dissolved in an EDTA solution, Ca^{2+} concentration was determined to be 10.6 ± 0.1, F^- 22.9 ± 0.1 and APRB 0.233 ± 0.012 μmol per mg of solid when APRB reagent was used as the hybridization reactant. Thus, the molar ratio of Ca^{2+} to F^- and APRB in the material was calculated to be 1 : 2.16 : 0.022. Approximately 46 CaF_2 molecules captured only one of APRB in the hybrid material. From TGA of the APRB, CaF_2 and CFA materials (refer to the ESI,† Fig. S3), APRB appears to undergo a strong thermal decomposition between 250 and 600 °C. The weight loss of APRB is 26% around 250 °C, and 27% around 400 °C. The former may be due to the volatilization of the alkyl chain $–C_{12}H_{25}$, and the latter due to the decomposition of azonaphtholamide.[13] The weight loss of APRB in the CFA material was 12.5% between 250 and 600 °C. Therefore, the mass percentage of APRB in the hybrid material was calculated to be 18.1%, *i.e.* the molar ratio of APRB to CaF_2 being approximately 1 : 40 is confirmed.

From the XRD data of CaF_2 and CFA (refer to the ESI,† Fig. S4), APRB has not altered the crystallization process of CaF_2, *i.e.* APRB was captured *via* the affinity between CaF_2 and the $–SO_3^-$ groups of the APRB.[14] From the SEM and HRTEM images (Fig. 2), the CaF_2-only particles are square shaped, with mutual adhesion, most of which are about 100 nm (Fig. 2 A–C). This is attributed to the dense packing of CaF_2 layers. The CFA particles are universally 100–200 nm in size with clear particle borderlines (Fig. 2 E). Therefore, the participation of APRB inhibited the self-stacking of CaF_2. Without doubt, the addition of APRB plays an important role in controlling the size and

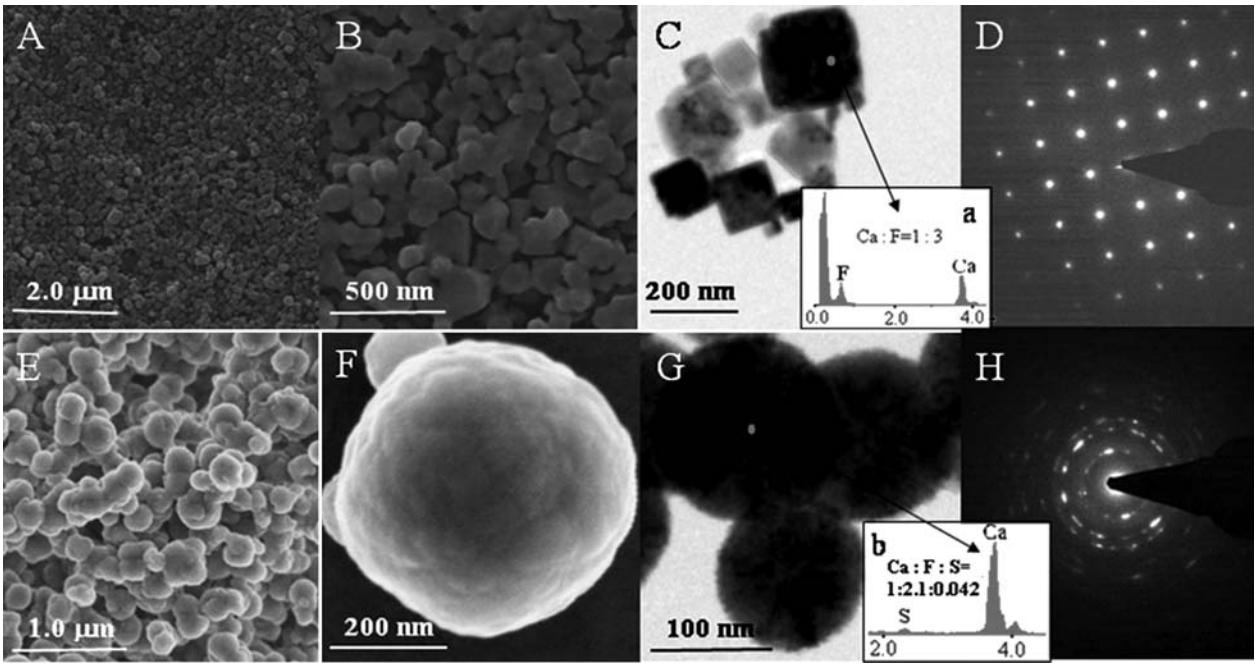

Fig. 2 SEM images of CaF_2-only (A, B) and CaF_2–APRB hybrid particles (E, F), HRTEM of CaF_2-only (C), CaF_2–APRB hybrid particles (G) and XRD images of CaF_2-only (D) and CaF_2–APRB hybrid particles (H).

morphology of the material. From XRD of the CaF_2 and CFA materials (Fig. 2 D,H), APRB resulted in poly-crystal formation, *i.e.* APRB was occluded in CaF_2. The IR spectrum (refer to the ESI,† Fig. S5) revealed the difference in composition between the CaF_2 and the CFA materials. The CaF_2 has characteristic vibration bands, strong peaks at 2954 and 2923 cm^{-1}, peaks at 1463 and 1377 cm^{-1} and a weak peak at 722 cm^{-1} (refer to the ESI,† Fig. S5 A). In the hybrid material, the characteristic vibration peaks of APRB were found at 3000–3600 cm^{-1} of O–H and N–H, 1650 cm^{-1} of C═O, 1500 cm^{-1} of N═N and the $\nu(-SO_3^-)$ peaks at 1230 and 1100 cm^{-1}.[15] It confirmed the hybridization of APRB into the growing calcium flouride. The molar ratio of Ca to F is 1 : 3 from the EDX data of CaF_2 (Fig. 2 C) where the excess of F^- may be adsorbed in the solid material for maintaining the charge equilibrium. From the EDX data of the CFA material (Fig. 2 G), the molar ratio of Ca to F and S was calculated to be 1 : 2.1 : 0.042. It indicated that 48 molecules of CaF_2 bound one APRB molecule, being identical with the above results.

In fact, APRB can react with Ca^{2+} by the affinity of sulfonic groups to form an insoluble Ca–APRB compound. However, the presence of F^- immediately captured the Ca from the Ca–APRB complex to form the CaF_2 protective cover, because the solubility coefficient (K_{sp}) of CaF_2 is much less than that of the Ca–APRB compound.[14b] APRB was released as a sandwich layer occluded into CaF_2 particles. Thus, the CFA material carried lots of negative charge supplied by APRB. This has been confirmed by the measurement of ζ-potentials: −22.4 mV for the CFA material and only −10.5 mV for CaF_2-only. Without doubt, the CFA material may be used to adsorb cationic organic compounds.

Structure of CASCA adsorbent

As is well known, it is difficult to separate nano-sized materials from a liquid. The practicality of the material becomes poor, even if it is highly effective in the adsorption of pollutants. In order to make better use of the hybrid material in the treatment of organic wastewater and remediation of a water body, the milli-sized adsorbent, CASCA, was prepared according to the recommended procedure. The optimal mass ratio of CFA material to sodium alginate is 1 : 1 (refer to the ESI,† Fig. S6). The instantaneous cross-linking of the interfacial alginate chains by calcium ions leads to a protective membrane which prevents APRB from going out of the beads. The beads are red globes, and their is size uniform, with a diameter of approximately 2 mm (Fig. 3 A) after aging for 1 h (refer to the ESI,† Fig. S7). From SEM images (Fig. 3 B,C), the outer surface of the calcium alginate ball after water loss is uneven, like water waves. There are a large number of folds like the cicada's wings (wall thickness less than 50 nm) within the sphere, which formed many high-capacity irregular pores (Fig. 3 D,E). By comparison of the SEM images (Fig. 3), the surface of the milli-sized globe is creased, being different from the smooth and regular calcium alginate (Fig. 3 A,D).[16] Furthermore, the target ball changes little in surface structure (Fig. 3 F). However, it can be found that many nano-sized CFA globes were captured by calcium alginate folds in the internal structure, and adhered together firmly (Fig.3 G–I). The results indicated that nano-sized CFA globes have been successfully loaded into the calcium alginate. By comparison of the BET surface area, pore size, and pore volume results (refer to the ESI,† Table S1), the BET surface area of CASCA decreased and neared that of CA when CFA was loaded into CA. However, the pore size of CASCA is similar to that of CFA, which is much more than that of CA. In addition, the trend of N_2 adsorption/desorption isotherms of CASCA is similar to that of CFA, while CA exhibits irregular isotherm curves (refer to ESI,† Fig. S8). Thus, CASCA retains the functional advantage of CFA.

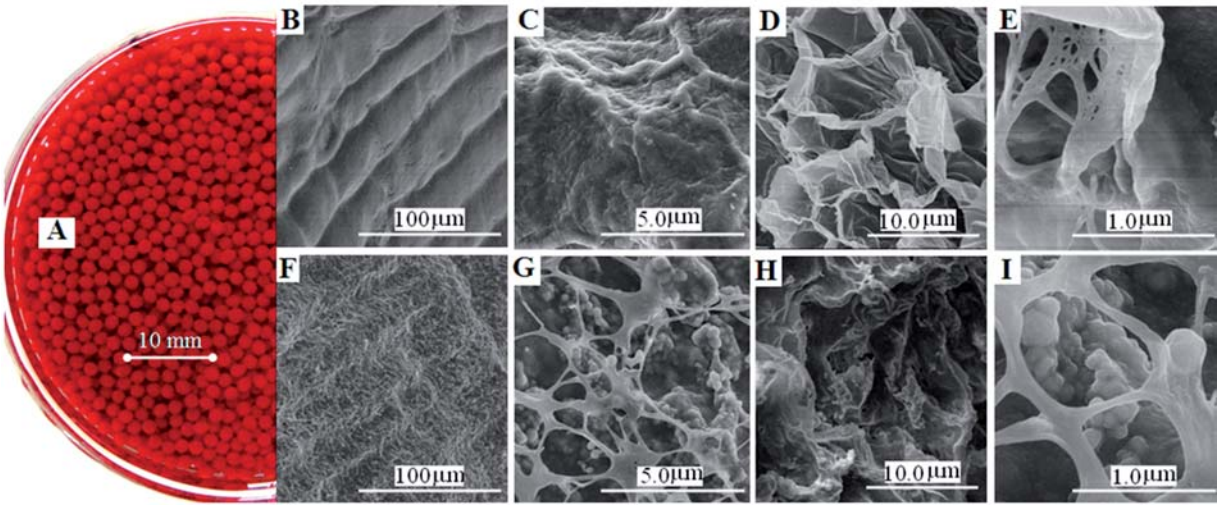

Fig. 3 Photograph of CASCA (A), and SEM of CA-only (the surface of B, C and the internal of D, E) and CASCA (the surface of F, G and the internal of H, I).

Interactions of dyes, PCBs and MC-LR with the materials

In order to investigate the adsorption capacity and selectivity of the CFA material, five cationic dyes (CR3R, BBBO, MB, VBB and EV) and five anionic ones *e.g.* RBRX-3B, WAGGS, RBRK-2BP, ABB6B, and MB-9 were used (refer to the ESI,† Fig. S9). The material can adsorb the cationic dyes selectively because it contains the active component, *i.e.* anionic APRB.[17] Therefore, four cationic dyes: CR3R, BBBO, MB and EV were selected for investigating the adsorption performance and mechanism of the CFA material, where the concentration of the dyes was determined by spectrophotometry. From the curves in Fig. 4, the molar ratios (γ) of BBBO, CR3R, MB and EV adsorbed to the APRB hybridized in the material increase with increasing initial concentrations (c_{L0}) of cationic dyes, and then all approach saturation at 2 when $c_{L0} > 180$ mmol L^{-1}. It confirms that such an adsorption is due to the ionic pair interaction between the cationic dye and APRB, *i.e.* $[(CaF_2)_m(APRB)_n]^{2n-} + 2nL^+ = L_{2n}[(CaF_2)_m(APRB)_n]\downarrow$ (L: CR3R, BBBO, EV and MB, $m = 46n$). The adsorption is complete in 15 min (refer to the ESI,† Fig. S10), hardly affected by pH greater than 3 (refer to the ESI,† Fig. S11) and electrolyte concentrations less than 0.2 mol L^{-1} (refer to the ESI,† Fig. S12), but it is affected by temperature for BBBO (refer to the ESI,† Fig. S13). From the images in Fig. 5, the milli-sized adsorbent of CASCA exhibits a high adsorption capacity for CR3R and VBB (bath 2), while little amounts of them were adsorbed by CA (bath 3). On the contrary, the WAGGS and RBRK-2BP were hardly captured (refer to the ESI,† Fig. S14). The saturation time of cationic dye is about 2 h on the milli-sized absorbent (refer to the ESI,† Fig. S15), which is much longer than that with CFA (refer to the ESI,† Fig. S10). A possible reason is the obstacle effect of calcium alginate on the entry of dye molecules. The adsorption capacity of the milli-sized adsorbent is 4 times as high as the CA (refer to the ESI,† Fig. S15). This is due to the supporting of the nano-sized CFA material. In addition, the milli-sized adsorbent remains highly effective when the pH is more than 3, temperature is between 10 and 60 °C and electrolyte concentration is less than 0.2 mol L^{-1} (refer to the ESI,† Fig. S16). From curve 1 in Fig. 6 A, the adsorption amount (γ) of CR3R on the milli-sized absorbent increases strongly and then gently with increasing concentration of CR3R. It indicates that a chemical adsorption may occur.

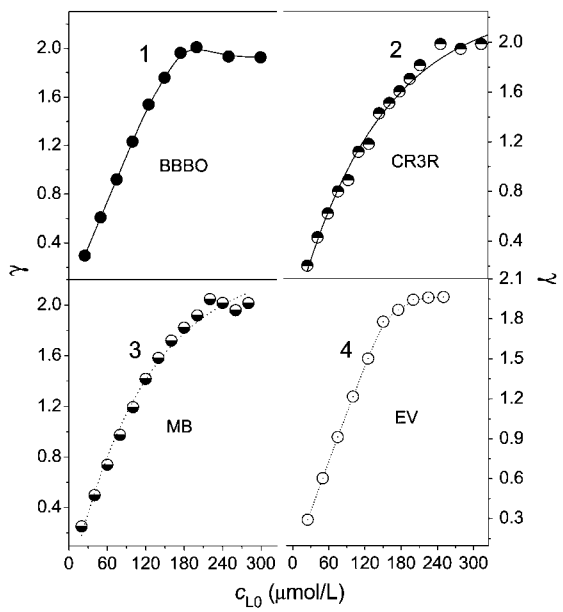

Fig. 4 Plots *vs.* c_{L0} of BBBO (A), CR3R (B), MB (C) and EV (D) when CFA (0.04%) was added.

As well as the negative charge, APRB contains a long alkyl chain, $-C_{12}H_{25}$ group, which may be exposed on the outside surface of the hybrid material. The hydrophobic shell formed will adsorb lipophilic organic substances *e.g.* POPs. Recently, POPs, which can be detected in a variety of surface waters,[18] have had impacts due to human and animal carcinogenic, teratogenic, and mutagenic toxicity.[19] They are also endocrine disruptors.[20] POPs are highly resistant in water environments. Despite that, their industrial use in many industrialized countries has been restricted since the 1970s. These compounds have also been considered for

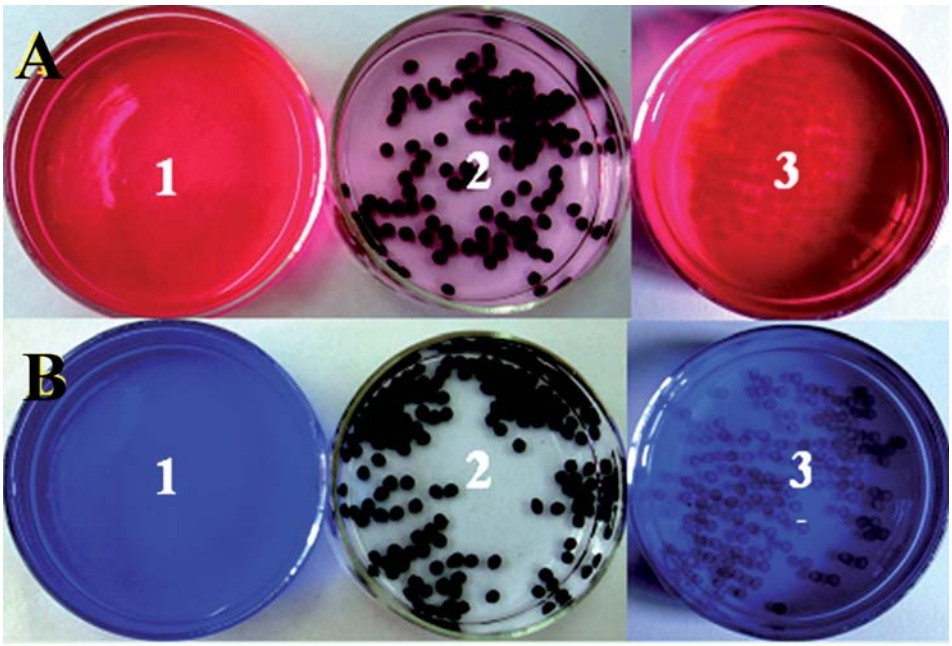

Fig. 5 Photos illustrating color change of dye supernatants: CR3R (A), VBB (B). All dyes were added initially in 40.0 μmol/L. 1: dye solution; 2: treated by adding 1.0 g (wet weight) of CASCA, 3: treated by adding 1.0 g (wet weight) of CA-only. All liquids were oscillated for 3 h in a shaking table.

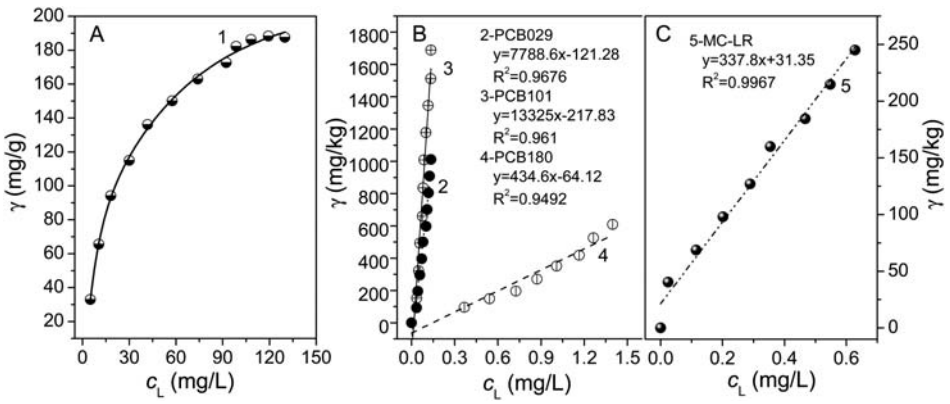

Fig. 6 Adsorptions of dyes (A), POPs (B) and M-LR (C). From 1 to 5: CR3R, PCB029, PCB101, PCB180 and MC-LR. The contents of the CASCA adsorbent are 0.06% for dyes, 0.23% for PCB029, 0.14% for PCB101 and PCB180, and 0.56% for MC-LR.

inclusion in the priority pollutant list of the State Environmental Protection Administration in China.[21] As a category of POPs, the adsorptions of three PCBs: PCB029, PCB101 and PCB180, were investigated on the milli-sized adsorbent. Unlike the cationic dye (Fig. 6 A), the γ values of PCBs increase linearly and have no equilibrium tendency. The adsorption of PCBs on the milli-sized absorbent accorded with the octanol–water partition law, *i.e.* the hydrophobic interaction occurred between the long alkyl chain of APRB and PCBs. According to the line slopes, the partition coefficients (K_{pw}) of PCBs were calculated to be 7788.6 mg kg^{-1} for PCB029, 13325 mg kg^{-1} for PCB101, and 434.6 mg kg^{-1} for PCB180. The K_{pw} values of PCB029 and PCB101 are much more than those (1666.7 and 7997.2 mg kg^{-1}) in the hybrid material (refer to the ESI,† Fig. S17 A) and directly proportional to their K_{ow} (log K_{ow} = 5.81 for PCB029 and 6.50 for PCB101).[22] This indicated that calcium alginate also plays an adsorption role for PCB029 and PCB101, as well as the hybrid material supported. However, K_{pw} of PCB180 in the milli-sized sorbent is much less than that (14041 mg kg^{-1}) in the hybrid material. The steric hindrance effect may lead to the uneasy entry of PCB180 into the milli-sized adsorbent.

In the last decade, toxic cyanobacterial blooms have often occurred worldwide in eutrophic lakes, rivers and reservoirs.[23] Microcystins are the most frequently occurring class of cyanotoxins, of which MC-LR is the most toxic and frequently detected congener.[24] It is produced by blue-green algae (*i.e.*, cyanobacteria) and may cause serious health problems for humans, such as irritation of the skin (dermatotoxins), cell damage (cytotoxins), liver damage (hepatotoxins), and damage to the nervous system (neurotoxins).[25] The concentration of dissolved MC-LR in the environment varies from trace up to 1800 μg L^{-1} or higher.[26] From the structure of MC-LR (refer to the ESI,† Fig. S18), it contains many polar (*e.g.* –NHR, –COOH) and non-polar groups (–CH_3, phenyl branched chain).

Furthermore, the inter-twist of the long MC-LR molecule may occur with the components in the adsorbent. As a representative of algae toxins, we tried to remove MC-LR from polluted water with the milli-sized CASCA. From curve 5 in Fig. 6 C, the adsorption amount (γ) of MC-LR increases linearly with increases of its equilibrium concentration. It indicated that MC-LR accorded with the octanol–water partition law. The hydrophobic stacking among the branched chain

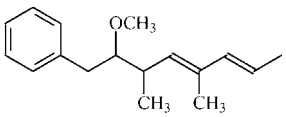

of MC-LR and the long alkyl chain of APRB may be the primary interaction form.[27] The K_{pw} of MC-LR in the CASCA adsorbent was calculated to be 369.2 mg kg^{-1} from the line slope (Fig. 6 C). Similar to PCB180, the K_{pw} is much less than that (3361 mg kg^{-1}) in the CFA material (refer to the ESI,† Fig. S17 B). For the same reason, this is due to the steric hindrance effect of MC-LR.

Application in polluted water treatment

The recycling and reuse of waste has attracted people's attention more and more.[28] A more practical hybrid material was prepared with an APRB-containing wastewater instead of the APRB reagent, and then it was used to prepare the milli-sized CASCA. With the same determination method, it contains a similar mole number of APRB to that prepared with the above APRB reagent. The milli-sized CASCA was used to treat two cationic dye wastewaters, a PCB-polluted water and an MC-LR–PCB mixture polluted water. From change of the column height (Fig. 7 A,B), the color strength and COD of two dye wastewaters obviously decreased with increase of the adsorbent—8.0 g of the wet adsorbent, *i.e.* approximately 0.45 g of dry weight, was added in 20.0 mL of the dye wastewater. The color strength of wastewater #1 decreased from 138000 to 27000 (Fig. 7 A), and the COD decreased from 3320 mg L^{-1} to only 850 mg L^{-1} (Fig. 7 B). The color strength of dye wastewater #2 decreased from 46500 to only 1870, and the COD decreased from 1200 mg L^{-1} to only 160 mg L^{-1}. Hence, the milli-sized CASCA has a good treatment effect for cationic dye wastewater, and was also simple to separate from the liquid.

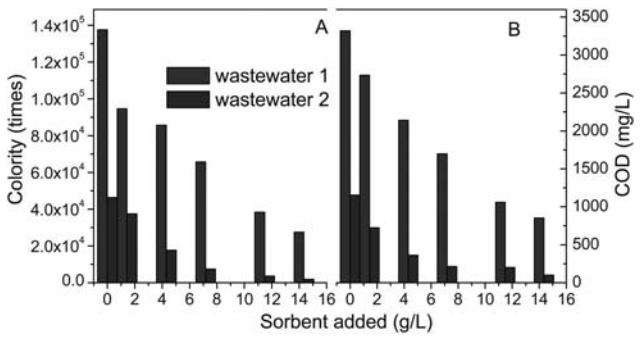

Fig. 7 Changes of color strength (A) and COD (B) in two dye wastewaters, sampled from: #1 - Jinjiang Chemicals, and #2 - Xingwu Dye Plant, when treated with CASCA (wet weight).

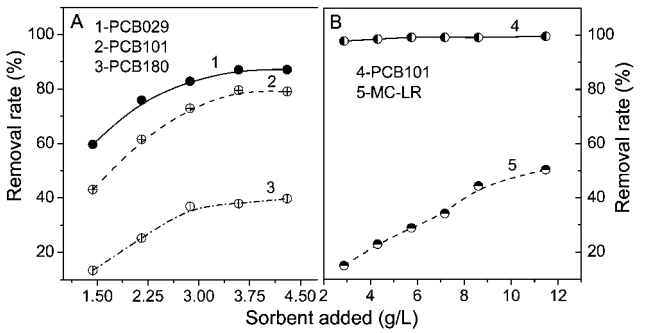

Fig. 8 Adsorptions of PCBs and MC-LR when the polluted waters (A: #3 and B: #4) were treated with CASCA.

In addition, two polluted waters with PCBs and MC-LR were treated by the milli-sized adsorbent. From the curves in Fig. 8 A, the removal rates of PCBs in the polluted water 3# containing PCB029, PCB101 and PCB180 increased with increase of the adsorbent. The removal rates are 85% for PCB029, 80% for PCB101 and 40% for PCB180 when more than 1.0 g of the wet adsorbent is added in 10.0 mL of the polluted water. For the treatment of the polluted water #4, containing PCB101 and MC-LR, the removal rate of MC-LR increased up to 50% with increase of the amount of adsorbent, as seen in curve 5 in Fig. 8 B, while that of PCB101 remains at approximately 100% (curve 4). Therefore, the co-existence of organic contaminants doesn't affect their simultaneous removal from polluted water. Without doubt, the adsorptions of dyes, PCBs and MC-LR in the polluted water are due to both the calcium alginate carrier and the CFA material combined into the milli-sized adsorbent. A comparison of the removal rates of colored substances and COD in the two dye wastewaters and that of PCBs and MC-LR in the two polluted waters when treated with the CFA material, CA and the milli-sized CASCA is shown in Fig. 9. From the column height (Fig. 9 A,B), the milli-sized CASCA is better than the others in the removal of the color substances and COD. However, the

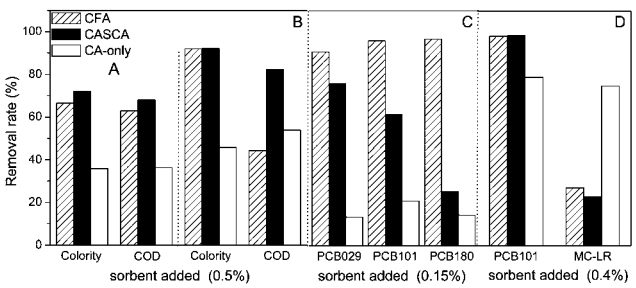

Fig. 9 Change of the removal rate of color strength and COD of two kinds dye wastewaters (A: #1 and B: #2) when treated with 0.5% of the three materials (dry weight). 20.0 mL of wastewater #1 or #2 and 3.6 g wet weight CASCA or 8.0 g wet weight CA-only were oscillated in a shaking table for 3 h. 10.0 mL of wastewater #1 or #2 was treated with 0.5% CFA. C: Change of the removal rate of PCBs in the polluted water (#3) when treated with 0.15% of three materials (dry weight), where the initial concentration is 2.4 mg L^{-1} PCB029, 2.0 mg L^{-1} PCB101 and 2.0 mg L^{-1} PCB180. D: The removal rate of PCBs and MC-LR in the polluted water (#4) when treated with 0.4% of the materials (dry weight), where the initial concentrations are 2.0 mg L^{-1} PCB101 and 2.0 mg L^{-1} MC-LR.

milli-sized CASCA is inferior to the CFA material in the adsorption of PCB mixtures (especially for PCB180), but much better than the calcium alginate (Fig. 9 C). For treatment of the PCB and MC-LR mixture, the milli-sized CASCA has the same PCB101-adsorbing affect (100%) as the CFA material (Fig. 9 D). However, CA has the highest removal rate of MC-LR. Because the molecular size of MC-LR ($1.2 \times 1.4 \times 1.8$ nm)[29] approximates to the pore size of CA (refer to the ESI,† Table S1), the adsorption of MC-LR on CA becomes firmer. Owing to the high adsorption capacity of the milli-sized CASCA for POPs and cationic organic substances, it may be made into a drift blanket enclosed in a light-thin foam board for spreading on the surface of a polluted water body, or immobilizing at the bottom of an artificial floating island, or fixing onto a ship's bottom, for the *in situ* cleaning of lipophilic POPs, environmental hormones, hydrophilic algae toxins and arylamine compounds (Fig. 1 D). Thus, the *in situ* restoration of a polluted water body and the waste resource, *e.g.* "using waste to treat waste" becomes possible.

Conclusion

A new-style, highly effective material was prepared by the hybridization of APRB into calcium fluoride and characterized structurally by various instruments. In order to achieve wide engineering use, *e.g.* simple solid–liquid separation, a milli-sized CASCA material was prepared with calcium alginate supporting the CFA hybrid and its adsorption capacity was determined for cationic dyes, PCBs and MC-LR. The selective adsorption of cationic dyes corresponded to the chemical adsorption *via* charge attraction, and that of PCBs and MC-LR to the octanol–water partition law *via* hydrophobic stacking. The effects of pH, ionic strength, temperature and time have been investigated in detail. The milli-sized adsorbent was used to treat two dye wastewaters and two polluted waters with satisfactory results. In the preparation process of the adsorbent, all of the reactants are easily available and harmless to the environment, and also a concentrated APRB-containing wastewater was reused instead of APRB reagent. Therefore, this work has developed a simple, eco-friendly and practical method for the large-scale production of a cost-effective sorbent.

Acknowledgements

We thank the the National Key Technology R&D Program of China (Grant No. 2006BAJ08B10) and the National S&T Major Project of China (Grant No.2008ZX07421-002) for financially supporting this work.

Notes and references

1 (*a*) X. H. Qiu, T. Zhu, J. Li, H. S. Pan, Q. L. Li, G. F. Miao and J. C. Gong, *Environ. Sci. Technol.*, 2004, **38**, 1368–1374; (*b*) G. J. Zheng, A. O. W. Leung, L. P. Jiao and M. H. Wong, *Environ. Int.*, 2008, **34**, 1050–1061.

2 G. J. Hu, C. Sun, J. Li, Y. G. Zhao, H. Wang and Y. Q Li, *Ecotoxicology*, 2009, **18**, 647–651.

3 (*a*) E. Heinisch, A. Kettrup, W. Bergheim and S. Wenzel, *Fresenius Environ. Bull*, 2004, **15**, 148–169; (*b*) K. Hilscherova, K. Kannan, H. Nakata, N. Hanari, N. Yamashita, P. W. Bradley, J. M. McCabe, A. M. Taylor and J. P. Giesy, *Environ. Sci. Technol.*, 2003, **37**, 468–474; (*c*) K. E. Havens, T. James, T. L. East and V. H. Smith, *Environ. Pollut.*, 2003, **122**, 379–390.

4 (*a*) S. Xu, X. Jiang, X. Wang, Y. Tan, C. Sun, J. Feng, L. Wang, D. Martens and B. M. Gawlik, *Bull. Environ. Contam. Toxicol.*, 2000, **64**, 176–183; (*b*) L. F. Ping, Y. M. Luo, H. B. Zhang, Q. B. Li and L. H. Wu, *Environ. Pollut.*, 2007, **147**, 358–365; (*c*) Z. W. Tang, Z. F. Yang, Z. Y. Shen, J. F. Niu and E. F. Liao, *Arch. Environ. Contam. Toxicol.*, 2007, **53**, 303–312; (*d*) J. Z. Ni, Y. M. Luo, R. Wei and X. H. Li, *Eur. J. Soil Sci.*, 2008, **59**, 1020–1026.

5 (*a*) B. L. Yuan, Y. B. Li, X. D. Huang, H. J. Liu and J. H. Qu, *J. Photochem. Photobiol., A*, 2006, **178**, 106–111; (*b*) P. Pendleton, R. Schumann and S. H. Wong, *J. Colloid Interface Sci.*, 2001, **240**, 1–8.

6 M. Yang, J. W. Yu, Z. L. Li, Z. H. Guo, M Burch and T. F. Lin, *Science*, 2008, **319**, 158.

7 (*a*) A. Christensen, M. D. Gurol and T. Garoma, *Water Res.*, 2009, **43**, 3910–3921; (*b*) A. Bahdod, S. E. Asri, A. Saoiabi, T. Coradin and A. Laghzizil, *Water Res.*, 2009, **43**, 313–318; (*c*) K. M. Smith, G. D. Fowler, S. Pullket and N. J. D. Graham, *Water Res.*, 2009, **43**, 2569–2594.

8 (*a*) I. M. Banat, P. Nigam, D. Singh and R. Marchant, *Bioresour. Technol.*, 1996, **58**, 217–227; (*b*) B. W. Atkinson, F. Bux and H. C. Kasan, *Water SA*, 1998, **24**, 129–135; (*c*) G. Crini, *Bioresour. Technol.*, 2006, **97**, 1061–1085; (*d*) T. Robinson, G. McMullan, R. Marchant and N. Poonam, *Bioresour. Technol.*, 2001, **77**, 247–255; (*e*) K. Vijayaraghavan and Y. S. Yun, *Biotechnol. Adv.*, 2008, **26**, 266–291.

9 (*a*) V. Gómez, M. S. Larrechi and M. P. Callao, *Chemosphere*, 2007, **69**, 1151–1158; (*b*) G. Crini and P. M. Badot, *Prog. Polym. Sci.*, 2008, **33**, 399–447; (*c*) W. Z. Liu, F. Huang, Y. Q. Liao, J. Zhang, G. Q. Ren, Z. Y. Zhuang, J. S. Zhen, Z. Liu and C. Wang, *Angew. Chem., Int. Ed.*, 2008, **47**, 5619–5622.

10 (*a*) S. A. Ong, K. Uchiyama, D. Inadama and K. Yamagiwa, *J. Hazard Mater.*, 2009, **165**, 696–703; (*b*) N. Cottin and G. Merlin, *Chemosphere*, 2008, **73**, 711–716; (*c*) F. P. van der Zee and S. Villaverde, *Water Res.*, 2005, **39**, 1425–1440; (*d*) K. Thangavadivel, M. Megharaj, R. S. C. Smart, P. J. Lesniewski and R. Naidu, *J. Hazard. Mater.*, 2009, **168**, 1380–1386; (*e*) M. Li, Y. J. Wu, Z. L. Yu, G. P. Sheng and H. Q. Yu, *Water Res.*, 2009, **43**, 1247–1256.

11 (*a*) S. Mintova, V. D. Waele, U. Schmidhammer, E. Riedle and T. Bein, *Angew. Chem., Int. Ed.*, 2003, **42**, 1611–1614; (*b*) Q. F. Zhang, T. P. Chou, B. Russo, S. A. Jenekhe and G. Z. Cao, *Angew. Chem., Int. Ed.*, 2008, **47**, 2402–2406; (*c*) A. C. Templeton, W. P. Wuelfing and R. W. Murray, *Acc. Chem. Res.*, 2000, **33**, 27–36; (*d*) C. J. Zhong and M. M. Maye, *Adv. Mater.*, 2001, **13**, 1507–1511; (*e*) J. Genzer and K. Efmenko, *Science*, 2000, **290**, 2130–2133; (*f*) H. Nobukuni, Y. Shimazaki, F. Tani and Y. Naruta, *Angew. Chem., Int. Ed.*, 2007, **46**, 8975–8978.

12 (*a*) J. Lin and H. W. Gao, *J. Mater. Chem.*, 2009, **19**, 3598–3601; (*b*) D. H. Zhao, Y. L. Zhang, Y. P. Wei and H. W. Gao, *J. Mater. Chem.*, 2009, **19**, 7239–7244.

13 (*a*) C. C. Ribeiro, C. C. Barrias and M. A. Barbosa, *Biomaterials*, 2004, **25**, 4363–4373; (*b*) A. K. Pandey, S. D. Pandey, V. Misra and S. Devib, *J. Hazard. Mater.*, 2003, **98**, 177–181; (*c*) H. G. Park and M. Y. Chae, *J. Chem. Technol. Biotechnol.*, 2004, **79**, 1080–1083; (*d*) R. P. Dhakal, K. N. Ghimire, K. Inoue, M. Yano and K. Makino, *Sep. Purif. Technol.*, 2005, **42**, 219–225; (*e*) C. Jeon, J. Y. Park and Y. J. Yoo, *Biochem. Eng. J.*, 2002, **11**, 159–166.

14 (*a*) H. P. Cong and S. H. Yu, *Adv. Funct. Mater.*, 2007, **17**, 1814–1820; (*b*) D. H. Zhao and H. W. Gao, *Environ. Sci. Pollut. Res.*, 2010, **17**, 97–105.

15 E. Pretsch, P. Bühlmann and C. Affolter, *Structure determination of organic compounds tables of spectral data*, Springer-Verlag Berlin Heidelberg, 2000.

16 G. Fundueanu, C. Nastruzzi, A. Carpov, J. Desbrieres and M. Rinaudo, *Biomaterials*, 1999, **20**, 1427–1435.

17 H. Y. Wang and H. W. Gao, *Environ. Sci. Pollut. Res.*, 2009, **16**, 339–347.

18 (*a*) H. Iwata, S. Tanabe, N. Sakai, A. Nishimura and R. Tatsukawa, *Environ. Pollut.*, 1994, **85**, 15–33; (*b*) X. H. Qiu, T. Zhu, J. Li, H. S. Pan, Q. L. Li, G. F. Miao and J. C. Gong, *Environ. Sci. Technol.*, 2004, **38**, 1368–1374; (*c*) G. J. Zheng, A. O. W. Leung, L. P. Jiao and M. H. Wong, *Environ. Int.*, 2008, **34**, 1050–1061; (*d*)

L. F. Ping, Y. M. Luo, H. B. Zhang, Q. B. Li and L. H. Wu, *Environ. Pollut.*, 2007, **147**, 358–365.
19 (*a*) P. C. Hsu, M. H. Pan, L. A. Li, C. J. Chen, S. S. Tsai and Y. L. Guo, *Toxicol. Appl. Pharmacol.*, 2007, **221**, 68–75; (*b*) P. C. Hsu, M. H. Li and Y. L. Guo, *Toxicology*, 2003, **187**, 117–126.
20 L. Ritter, K. R. Solomon and J. Forget, *Persistent organic pollutants: An assessment report on DDT, aldrin, dieldrin, endrin, chlordane, heptachlor, hexachlorobenzene, mirex, toxaphene, polychlorinated biphenyls, dioxins, and furans*, International Programme on Chemical Safety (IPCS) within the framework of the Inter-Organization Programme for the Sound Management of Chemicals (IOMC), Canadian Network of Toxicology Centers and Deloitte and Touche Consulting Group: Guelph, ON, Canada, 1995.
21 X. H. Bi, S. G. Chu, Q. Y. Meng and X. B. Xu, *Agric. Ecosyst. Environ.*, 2002, **89**, 241–252.
22 (*a*) K. B. Woodburn, W. J. Doucette and A. W. Andren, *Environ. Sci. Technol.*, 1984, **18**, 457–459; (*b*) W. J. Dulfer and H. A. J. Govers, *Chemosphere*, 1995, **30**, 293–306.
23 K. E. Havens, T. James, T. L. East and V. H. Smith, *Environ. Pollut.*, 2003, **122**, 379–390.
24 (*a*) J. Lee and H. W. Walker, *J. Membr. Sci.*, 2008, **320**, 240–247; (*b*) N. Gupta, S. C. Pant, R. Vijayarghavan and P. V. L. Rao, *Toxicology*, 2003, **188**, 285–296.
25 (*a*) N. Gupta, S. C. Pant, R. Vijayarghavan and P. V. L. Rao, *Toxicology*, 2003, **188**, 285–296; (*b*) M. G. Antoniou, A. A. de la Cruz and D. D. Dionysiou, *J. Environ. Eng.*, 2005, **131**, 1239–1243.
26 (*a*) K. Sivonen and G. Jones, Cyanobacterial toxins, in *Toxic Cyanobacteria in Water: A Guide to their Public Health Consequences, Monitoring and Management.*, ed. I. Chorus and J. Bartram, E and FN Spon, London/New York, 1999, pp. 41–111; (*b*) I. Chorus and J. Bartram, *Toxic Cyanobacteria in Water, A Guide to Public Health Consequences, Monitoring and Management*, E and FN Spon on behalf of WHO, London, 1999.
27 C. Donati, M. Drikas, R. Hayes and G. Newcombe, *Water Res.*, 1994, **28**, 1735–1742.
28 (*a*) F. M. Jin, J. Yun, G. M. Li, A. Kishita, K. Tohji and H. Enomoto, *Green Chem.*, 2008, **10**, 612–615; (*b*) A. Tal, *Science*, 2006, **313**, 1081–1084.
29 X. Feng, F. Rong, D. Fu, C. Yuan and Y. Hu, *Chin. Sci. Bull.*, 2006, **51**, 1191–1198.

